

ALPHA-NULL DEFOCUS: AN OPTIMUM DEFOCUS CONDITION WITH RELEVANCE FOR FOCAL-SERIES RECONSTRUCTION

Michael A. O'Keefe

National Center for Electron Microscopy, MSD, LBNL B72, Berkeley, CA 94720

DISCLAIMER

This document was prepared as an account of work sponsored by the United States Government. While this document is believed to contain correct information, neither the United States Government nor any agency thereof, nor The Regents of the University of California, nor any of their employees, makes any warranty, express or implied, or assumes any legal responsibility for the accuracy, completeness, or usefulness of any information, apparatus, product, or process disclosed, or represents that its use would not infringe privately owned rights. Reference herein to any specific commercial product, process, or service by its trade name, trademark, manufacturer, or otherwise, does not necessarily constitute or imply its endorsement, recommendation, or favoring by the United States Government or any agency thereof, or The Regents of the University of California. The views and opinions of authors expressed herein do not necessarily state or reflect those of the United States Government or any agency thereof, or The Regents of the University of California.

Ernest Orlando Lawrence Berkeley National Laboratory is an equal opportunity employer.

Ernest Orlando Lawrence Berkeley National Laboratory – LBNL-

ALPHA-NULL DEFOCUS: AN OPTIMUM DEFOCUS CONDITION WITH RELEVANCE FOR FOCAL-SERIES RECONSTRUCTION

Michael A. O'Keefe

National Center for Electron Microscopy, LBNL B72, Berkeley, CA 94720, USA

Two optimum defocus conditions are well known to users of high-resolution transmission electron microscopes. Scherzer¹ defocus is useful in high-resolution electron microscopy (HREM) because it produces an image of the specimen "projected potential" to the resolution of the microscope². Lichte³ defocus is useful in electron holography because it optimizes sampling in frequency-space by minimizing the slope of the microscope objective lens phase change out to the highest spatial frequency in the hologram, consequently minimizing dispersion. For focal-series reconstruction, the requirement to maximize transfer into the image of high-frequency diffracted beam amplitudes leads to a third optimum defocus condition⁴.

Image reconstruction methods allow the achievement of super-resolution – resolution beyond the native (Scherzer) resolution of the microscope – by correction of the phase changes introduced by the microscope objective lens⁵. One such method is focal-series reconstruction, in which diffracted-beam information obtained at several different focus values is combined⁶. To produce a valid super-resolution result, it is necessary to ensure that every spatial frequency is represented appropriately. Suitable choice of an optimum defocus produces optimum transfer of diffracted-beam amplitudes at any chosen spatial frequency.

Same-phase transfer of diffracted-beam amplitudes is maximized at Scherzer defocus, $\varepsilon_S = -\sqrt{(3C_S\lambda/2)}$, but only extends to the Scherzer resolution of $d_S = 0.64C_S^{1/4}\lambda^{3/4}$, where λ is electron wavelength and C_S is the objective lens spherical aberration coefficient. Mixed-phase transfer of diffracted-beam amplitudes can occur beyond Scherzer resolution, out to the microscope information limit⁷ of $d_\Delta = \sqrt{(\pi\lambda\Delta/2)}$. Here Δ is the standard deviation of microscope spread of focus occasioned by partial temporal coherence of the electron beam, $\Delta = C_C\sqrt{\{(\sigma^2(V)/V^2 + 4\sigma^2(I)/I^2 + \sigma^2(E)/E^2)\}}$, where $\sigma^2(V)$, $\sigma^2(I)$, $\sigma^2(E)$ are the variances in high-voltage, lens current and energy spread over the time scale of image acquisition, and C_C is the chromatic aberration coefficient of the objective lens. Although partial spatial coherence does not contribute to the information limit of the microscope, it does limit transfer of diffracted-beam amplitudes into any single image. The envelope for incident beam convergence has the form $E_\alpha(\mathbf{u}) = \exp\{-\pi^2\alpha^2(\varepsilon + \lambda^2 C_S \mathbf{u}^2)^2 \mathbf{u}^2\}$. For an incident beam convergence semi-angle⁸ of 1.3α , the cutoff spatial frequency is given by⁹

$$|\mathbf{u}|_\alpha = S_+^{1/3} + S_-^{1/3} \quad \text{where} \quad S_\pm = \left[\frac{3.3}{4\pi\alpha} \pm \sqrt{\frac{\varepsilon^3}{27C_S\lambda^2} + \left(\frac{3.3}{4\pi\alpha}\right)^2} \right] / C_S\lambda^2$$

Because the import of the above expression is obscure, it is more useful to consider the action of incident-beam convergence as a function of defocus, ε , for any particular spatial frequency, $|\mathbf{u}|$. The phase imposed on diffracted-beam amplitudes is $\chi(\mathbf{u}) = \pi\varepsilon\lambda|\mathbf{u}|^2 + \pi C_S\lambda^3|\mathbf{u}|^4/2$. Transfer of beam hkl varies with defocus as $\sin\{\pi\varepsilon\lambda|\mathbf{u}_{hkl}|^2\}$, with an offset from zero defocus of $\sin\{\pi C_S\lambda^3|\mathbf{u}_{hkl}|^4/2\}$. Incident-beam convergence confines this transfer to a Gaussian "packet" of defocus values centered on the alpha-null defocus. For a diffracted beam hkl , with a spatial frequency of \mathbf{u}_{hkl} , the envelope for incident beam convergence has null damping effect when defocus is $\varepsilon_\alpha^0(\mathbf{u}_{hkl}) = -C_S(\lambda\mathbf{u}_{hkl})^2$. On either side of this alpha-null defocus value, the damping effect of incident-beam convergence reduces the diffracted-beam transfer to $\exp(-2)$, or 13.5%, when defocus reaches a value of $\varepsilon_\alpha^0(\mathbf{u}_{hkl}) \pm \varepsilon_\alpha^{2\sigma}(\mathbf{u}_{hkl}) = -C_S(\lambda\mathbf{u}_{hkl})^2 \pm \sqrt{2}/(\pi\alpha\mathbf{u}_{hkl})$. Thus the position of alpha-null defocus for any particular spatial frequency depends only on the value of C_S – on the other hand, defocus-packet width around the alpha-null defocus depends only on the convergence semi-angle.

Focal-series reconstruction is facilitated when defocus-packets for all diffracted beams overlap. To image carbon atoms at the correct positions in a [110] "dumbbell" image from diamond, the super-resolution image must include contributions from four sets of diffracted beams out to the 004 spacing of 0.89\AA ¹⁰. Transfer at the four diffracted-beam frequencies is confined to four defocus packets centered on the alpha-null defocus of each spatial frequency. Over a defocus range of 0 to -5000\AA (fig.1), offsets of the defocus packets to their alpha-null positions are larger and their packet widths narrower (making overlap more difficult) for smaller spacings (higher frequencies). Reduction in C_S from 0.9mm (left column) to 0.6mm (right) reduces the alpha-null offset and improves overlap. Reduction in convergence from 1.0 milliradian (top row) to 0.5 milliradian (center) to 0.25 milliradian (bottom) increases packet widths and improves overlap.

Under NCEM OÅM (one-Ångström microscope¹¹) conditions, reconstruction gives a [110] diamond image with the correct 0.89Å spacing (fig.2a). With the effects of 20Å focus spread included (fig.2b), the alpha-null defocus (arrow) is seen as the optimum defocus for transfer of all diffracted information out to 0.89Å. The alpha-null defocus should be included as the (furthest underfocus) limit for all focal series reconstruction.¹²

1. O. Scherzer, J. Appl. Phys. **20** (1949) 20.
2. J.M. Cowley, and S. Iijima, Z. Naturforsch. 27a (1972) 445-451.
3. H. Lichte, *Ultramicroscopy* **38** (1991) 13.
4. Michael A. O'Keefe et al., *Ultramicroscopy* (2001) submitted.
5. M.A. O'Keefe, R&D Magazine (1999) <<http://www.rdmag.com/archives/basics/10microscopy.htm>>
6. W.M.J. Coene, A. Thust, M. Op de Beeck and D. Van Dyck, *Ultramicroscopy* **64** (1996) 109-135.
7. M.A. O'Keefe, *Ultramicroscopy* **47** (1992) 282-297.
8. Jan-Ölle Malm and Michael A. O'Keefe, in *51st Ann. Proc. MSA*, Cincinnati, Ohio (1993) 974-975.
9. M.A. O'Keefe and A. J. Pitt, *Electron Microscopy 1980*, The Hague, Netherlands, 122-123.
10. Y.C. Wang et al., *57th Ann. Proc. MSA*, Portland, Oregon (1999) 822-823.
11. M.A. O'Keefe, in *58th Ann. Proc. MSA*, Philadelphia, Pennsylvania (2000) 1036-1037.
12. Work supported by Director, Office of Science -- through the Office of Basic Energy Sciences, Material Sciences Division, of the U.S. Department of Energy, under contract No. DE-AC03-76SF00098.

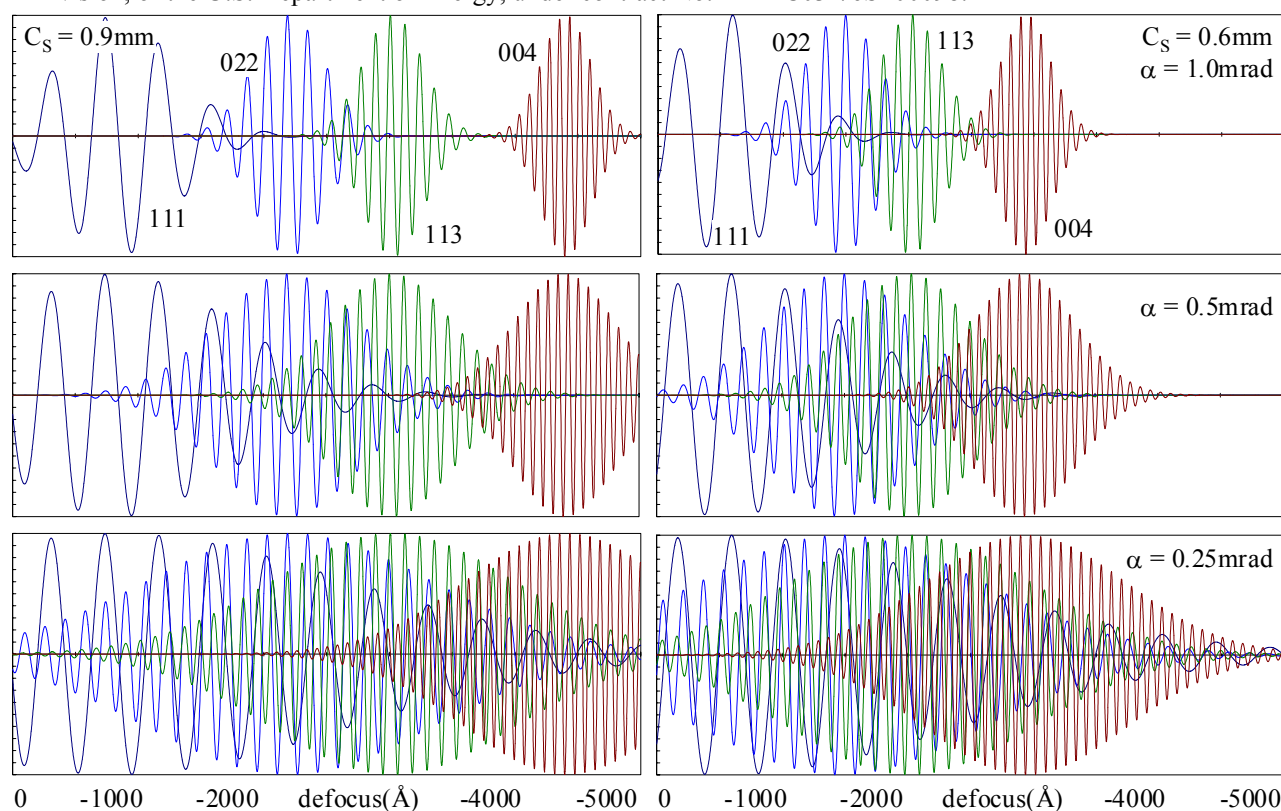


Fig.1 Defocus packets for decreasing spherical aberration C_s (across) and decreasing convergence α (down) show increasing transfer of [110] diamond diffracted beams. Plotted over the defocus range 0 to -5000\AA .

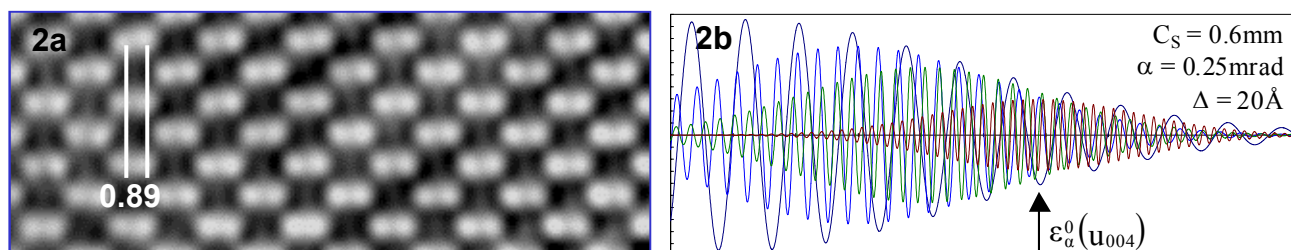


Fig.2. (a) Reconstruction from experimental OÅM focal series shows 0.89Å spacing of C-C “dumbbells”. (b) Under OÅM conditions transfer is optimized at the alpha-null defocus for the diamond 004 beam (arrow).